2010 IEEE International Conference on Robotics and Automation
Anchorage Convention District
May 3-8, 2010, Anchorage, Alaska, USA

High Sensitivity Initial Slip Sensor for Dexterous Grasp

Seiichi Teshigawara*, Kenjiro Tadakuma**, Aiguo Ming*, Masatoshi Ishikawa***, Makoto Shimojo*

Abstract— **Slip-detecting tactile sensors are essential for achieving human-like gripping motion with a robot hand. In previous research, we developed a flexible, thin and lightweight slip sensor that exploits the characteristics of pressure conductive rubber. However, using this sensor, it was difficult to distinguish between object slip and a change in the normal force. Therefore, in the present research, we investigated a method for identifying object slip by analyzing the frequency components of the output signal from the sensor. As a result, we found that high-frequency components of 1 kHz or more are included in the complex voltage signal generated by object slip. Therefore, by using this high-frequency component, we developed a simple sensor that distinguished between both contact and initial slip with high sensitivity.**

I. INTRODUCTION

Research and development of humanoid robots for assisting and supporting humans is currently being carried out at a number of research institutions. However, in order for robots to advance from laboratories and into human living spaces, robots must be able to adapt to their environment. For a humanoid robot to grasp an object, the robot's hand must have many degrees of freedom. Furthermore, using its hand, the robot must be able to grasp and operate a variety of objects. To perform such operations, tactile sensors are required to obtain information such as contact position, contact force, and slip. In particular, the sensation of slip is critical for a robot to grasp an object with minimal force, in order to prevent destruction of the object and allow the object to be operated dexterously [1].

Several attempts have been made to detect object slip by converting the change in a physical parameter into an electric signal. Howe et al. developed a sensor consisting of pairs of acceleration sensors arranged inside a silicon rubber sphere with a projection called a "nib"; this sensor detected vibrations on the surface of the sensor arising from initial slip [2]. Son et al. developed a sensor made up of four sheets of polyvinylidene fluoride (PVDF) film that were arranged in a semi-circular silicon rubber tube, which similarly detected vibrations caused by initial slip [3]. However, these sensors have problems in terms of miniaturization, weight reduction, and discrimination between contact, non-contact, and object slip for difficult objects. Maeno et al. modeled the structure of the human finger pad by finite element analysis, thus clarifying the properties of individual tactile receptors [4]. Then, Maeno et al. imitated the human gripping technique, developing sensors aligned inside a curved elastic surface at regular intervals along a strain gauge [5]. With this setup, they demonstrated the possibility of gripping an object of unknown weight and coefficient of friction. However, the number of wires and difficulty of miniaturization are problems, and the sensor can detect slip in only one direction. Shinoda et al. proposed a slip sensor with an Acoustic Resonant Tensor Cell (ARTC) [6]. The ARTC consisted of a resonance cavity within an elastic body and an ultrasonic receiving probe; stress in the slip direction was detected from changes in the resonance frequency of ultrasonic waves. However, the response and miniaturization of this sensor are problematic. Shimoyama et al. developed a micro warp gauge element by using microelectromechanical systems (MEMS) technology, and proposed a sensor that was capable of measuring force along three axes corresponding to the direction of the normal force and the shearing force [7]. This sensor has been successfully miniaturized, and its utility is high. However, as the detection area is enlarged, the number of wires increases in proportion to the number of sensors. Moreover, a thick coating of protective material must be applied to the surface of the sensor, and the arrangement and number of sensors must be optimized for each finger. Therefore, when this sensor is installed in a robot hand, there are a number of difficulties.

On the other hand, in our laboratory, we have developed a thin (0.5 mm) and flexible slip sensor composed of pressure conductive rubber [8][9]. This sensor exploits the unusual resistance change that occurs when the pressure conductive rubber undergoes shear deformation (circle A in Fig. 1). However, it is difficult to separate the resistance change caused by the normal force and the resistance change caused by object slip. In other words, it is difficult to distinguish between a change in the normal force and object slip. Therefore, in this study, we developed a method that utilizes the complex resistance change that occurs immediately before object slip (circle B in Fig. 1). First, we propose a technique for separating the output signal caused by object slip from the output signal that arises from a changing normal force. Moreover, we evaluate the stability of the output in the case of differing initial normal forces and changing surface properties of an object. Finally, we describe an experiment on adjustment of the gripping force by a parallel hand.

*Mechanical Engineering and Intelligent Systems, The University of Electro-Communications, 1-5-1 Chofugaoka, Chofu-shi, Tokyo 182-8585, Japan

**Department of Mechanical Engineering, Graduate School of Engineering, Osaka University Building-M4 4F Rm. 406, 2-1 Yamadaoka, Suita, Osaka 565-0871, Japan

***Department of Information Physics and Computing, Graduate School of Information Science and Technology, The University of Tokyo, 7-3-1 Hongo, Bunkyo-ku, Tokyo 113-0033, Japan

978-1-4244-5040-4/10/$26.00 ©2010 IEEE

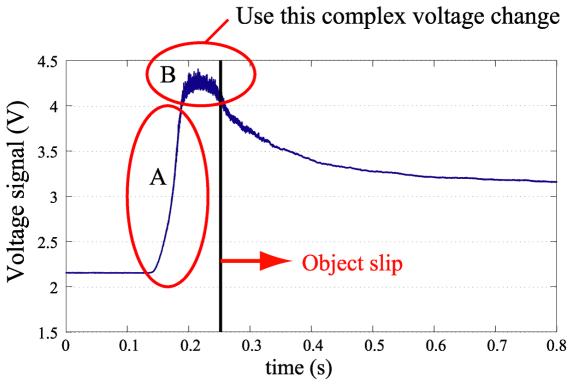

Fig. 1. Change in output from slip sensor

II. STRUCTURE OF SLIP SENSOR

The configuration of the proposed sensor is shown in Fig. 2 [9]. In the slip sensor, two electrodes are alternately coiled around a spiral structure, and pressure conductive rubber (6 mm×6 mm) rests on the electrodes. The electrode is connected to a DC power supply (5 V) through a resistance of 1 $k\Omega$. The voltage potential between the electrodes from the V_c terminal is converted into a digital signal, and signal processing is performed on a PC. Therefore, the sensor output is digital output that indicates whether or not the object slips. Since this sensor uses rubber, it is light-weight and low-profile (2.0 mm). We estimate that the minimum size of this sensor is 3 mm×3 mm×0.5 mm. Moreover, the structure of the sensor is extremely simple. As the detector plane becomes larger, the number of wires remains the same (only 4 wires are needed, including those for the power supply).

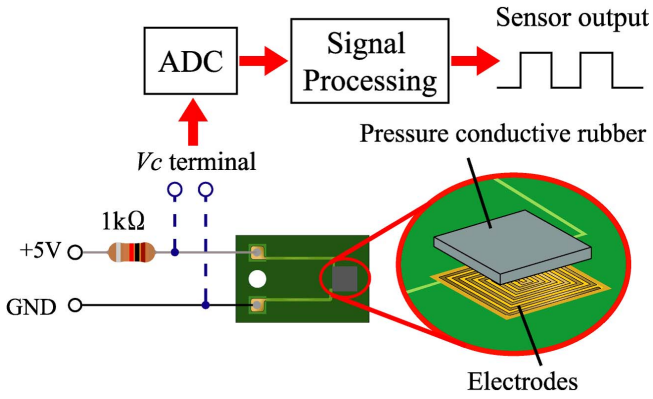

Fig. 2. Structure of slip sensor

III. SLIP SENSOR OUTPUT AND FREQUENCY ANALYSIS

We expect that signals of object slip and the normal force can be separated by frequency analysis of the complex fluctuations in the voltage potential signal between the electrodes (V_c) that occur when an object slips. Here, we examine this signal by applying the continuous wavelet transform (CWT). Furthermore, we compare the frequency observed for object slip with that observed for a change in the normal force, and describe the difference between the frequency components of the two.

A. Frequency components of object slip

The experimental apparatus is shown in Fig. 3. After placing the sensor on the horizontal plane, we put an acrylic plate over the slip sensor and applied a normal force by using the hemisphere pressure part. We set the normal force to 2 N by adjusting the position of the automatic Z-stage. Next, we attached a string between the edge of the acrylic plate and an automatic linear stage, through a load cell. We then slid the acrylic plate over the surface of the slip sensor. The sliding speed of the acrylic plate was set to 10 mm/s. We measured the voltage potential signal between electrodes (V_c) and the output from the load cell at a sampling frequency of 10 kHz.

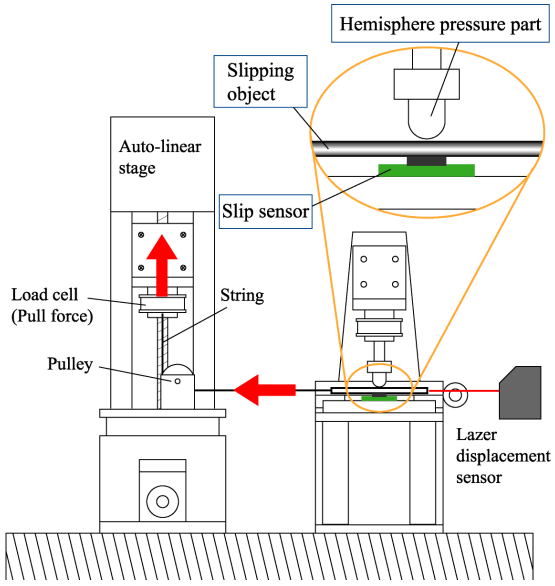

Fig. 3. Experimental apparatus: object slip generator

The experimental data is presented in Fig. 4. The vertical axis shows the output from the load cell and the voltage signal (V_c); the horizontal axis shows time. A change in tensile force was observed, which increased for 3 s and then became constant after the time marked with a vertical line. This change signifies the transition from static to kinetic friction. Therefore, the slip between the sensor surface and the acrylic plate occurs after the time marked by the vertical line. On the other hand, looking at the voltage signal (V_c), it can be seen that complex voltage fluctuations occurred immediately before the acrylic plate slides.

Next, we perform CWT of the voltage signal. The CWT constructs a time-frequency representation of signals that allows good time and frequency localization [10][11]. The results of the CWT are shown in Fig. 5. The upper panel shows the voltage signal, and the middle panel shows a CWT of the upper graph. The vertical axis shows the size of the mother wavelet, denoted as "scale". The smaller the wavelet scale is, the higher the frequency element. For example, scale 1 has a maximum frequency of about 5 kHz because the

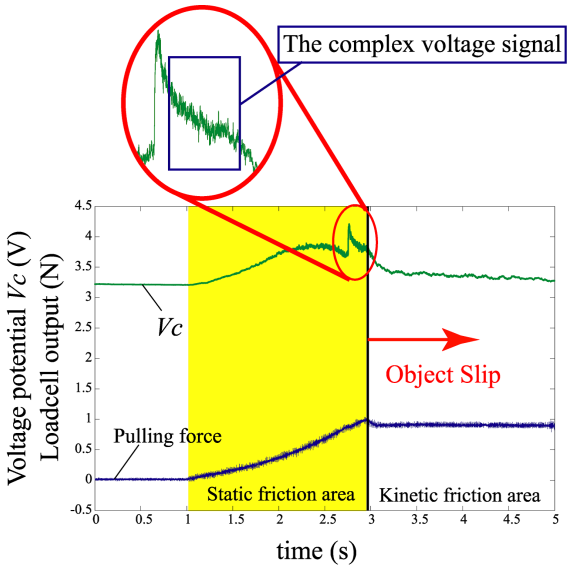

Fig. 4. Experimental results: output from slip sensor and the tensile force acting on the object

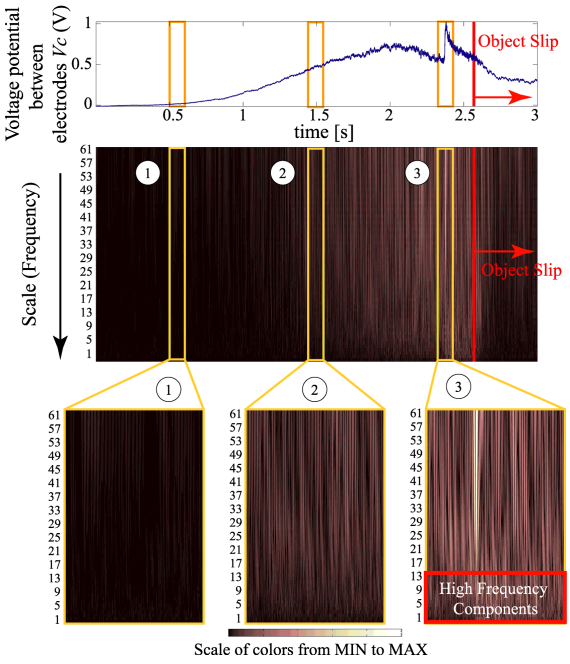

Fig. 5. CWT for object slip

sampling frequency is 10 kHz. Therefore, the upper side of the vertical axis shows low frequency, while the lower side shows high frequency. The color indicates the power of the frequency. The bottom three graphs are enlarged graphs of the rectangular areas in the middle frame. In the first stage of the voltage change due to the applied tensile force, few high-frequency components were observed and the power was also small. On the other hand, we found that the number of high-frequency components increased immediately before the plate began to slip, and high frequencies of 1 kHz or more appeared. This sensor can detect the initial slip by observing these high-frequency components.

B. Comparison with frequency components for change in normal force

Here, we compare the frequency components attributable to object slip with those associated with a change in the normal force. We perform a CWT of the voltage signal (V_c) for an increasing normal force. The experimental setup is shown in Fig. 6. We placed the sensor on a horizontal plane and put a 20 $mm \times 20$ mm acrylic plates over the sensor. Then, we applied a perpendicular load to the surface of the slip sensor, by using an automatic linear stage. We measured for the voltage signal between electrodes at this time and performed a CWT on the data.

The results of this experiment are shown in Fig. 7. We found that the highest frequency corresponding to a change in the normal force was about 600 Hz. High-frequency components did not appear when the normal force changed. From these results, it was found that the frequency components generated by object slip were higher than those generated by a change in the normal force. Therefore, it is possible to distinguish between object slip and the normal force by analyzing these frequency components.

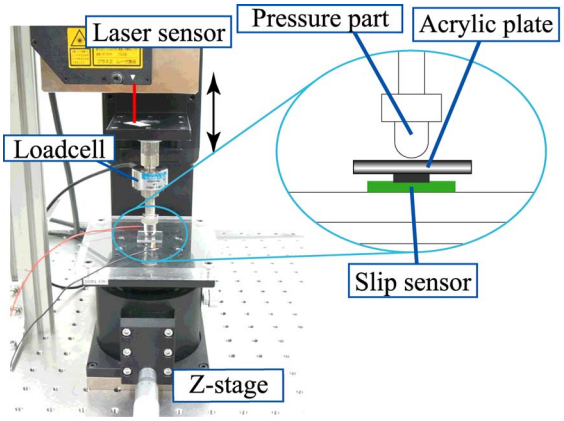

Fig. 6. Experimental setup: applying normal force

IV. SEPARATION METHOD USING DEFERENCE OF FREQENCY COMPONENT

From the experiments described above, we found that high-frequency components of 1 kHz or more are included in the complex voltage signal generated by object slip. In addition, these components have higher frequencies that those observed when only normal force is applied. In other words, it appears possible to distinguish object slip and from a change in the normal force by detection of these high-frequency components. Next, we describe in detail using the Discrete Wavelet Transform (DWT) as a method for detecting these transient high-frequency components.

A. Separation method using DWT

Here, we separate the normal force from the complex voltage signal from the V_c terminal by using the DWT as a high-pass filter. The DWT of the signal is calculated by passing the signal through a series of filters [10][11].

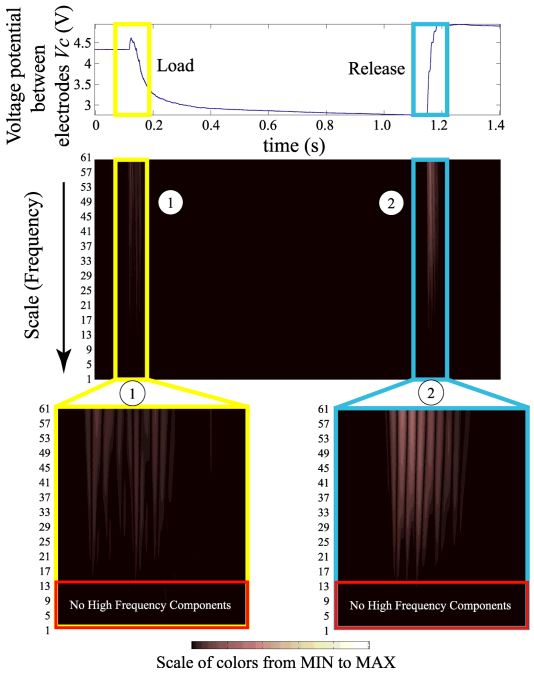

Fig. 7. CWT on output for loading and unloading

First, the samples are passed through a low-pass filter with impulse response g resulting in convolution. The signal is also decomposed simultaneously using a high-pass filter h. The outputs provide precise coefficients (from the high-pass filter) and approximation coefficients (from the low-pass filter).

In Section III, we found that frequency components of 1 kHz or higher are contained in the complex voltage signal. Therefore, we set the frequency band from 1 kHz to 5 kHz. The sampling frequency was 10 kHz, and the number of sampling points was 64 points/cycle. Level 1 DWT was performed on the data by using the Haar wavelet, which was employed to ensure a high speed of computation. Moreover, the peak-to-peak value was taken from the DWT result as the simple difference, and the threshold was set to a certain value. By setting a suitable threshold, a judgment can be made regarding the occurrence of object slip.

B. Establishing threshold and evaluating detection performance

We set the threshold by comparing the results of DWT on the voltage signals from the V_c terminal when only a change in the normal force occurred and when object slip occurred. Furthermore, we examined the effects of changing the initial normal force and the surface properties of the sliding object.

This time, we measured the voltage signal from the V_c terminal under the following conditions, and then performed DWT.

1) Applying only a normal force to the surface of the slip sensor.
2) Setting the initial normal force to 2 N, 3 N, or 4 N, and sliding the acrylic plate over the surface of slip sensor.
3) Changing the surface properties of the slipping object by using cloth, wood or paper, and sliding the material over the surface of the slip sensor.

The results obtained for condition 1 are shown in Fig. 8. The results obtained for condition 2 and condition 3 are shown in Figs. 9-11 and Figs.12-14, respectively. The upper panels show the voltage signal from the V_c terminal, and the lower panels show the results of DWT.

First, as shown in Fig. 8, when only the normal force changed, the wavelet coefficient exhibited little variation (Max:$\pm$0.005). On the other hand, in the other DWT results, for example, Fig. 9, it can be seen that the wavelet coefficient increased just before object slip occurred (Max: $\pm$0.04). Therefore, we found that the initial slip of the object could be separated from the normal force change by setting the threshold on the basis of to the DWT results. Accordingly, we set the threshold to $\pm$0.01.

Next, as shown in Figs. 9-11, the threshold was exceeded in a similar manner, even though the initial normal force was changed. As shown in Figs. 12-14, all DWT values exceeded the threshold. Thus, we can detect the slip of cloth, wood, and paper. When the object was cloth or paper, the wavelet coefficient became slightly smaller, which can likely be attributed to the frictional properties of the material. There is hardly any difference in the power of the wavelet coefficient when the initial normal force was set as 2 N, 3 N, and 4 N and when the surface properties of the sliding object were changed to cloth, wood, and paper. Therefore, even if the normal force changes and the surface properties of the object are changed, object slip can be detected by using the same threshold.

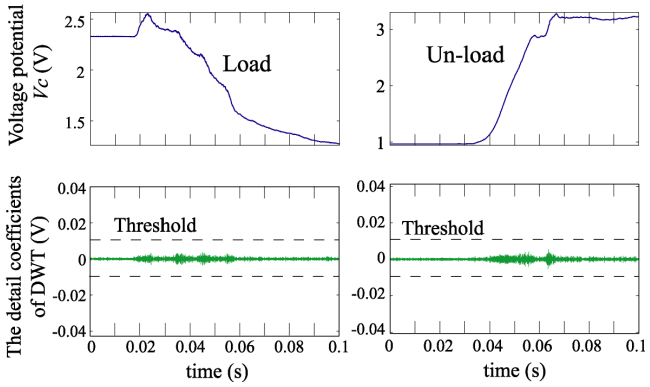

Fig. 8. Analysis results: DWT for loading and unloading

V. GRIPPING FORCE CONTROL BASED ON SLIP DETECTION

Using our previous slip detection algorithm, slip detection was difficult when the normal force changed. However, by using the new phenomenon confirmed in the present report, object slip is expected to be detected regardless of changes in normal force. We carried out an experiment on gripping force adjustment by using a parallel hand with installed slip sensors. This parallel hand is shown in Fig. 15.

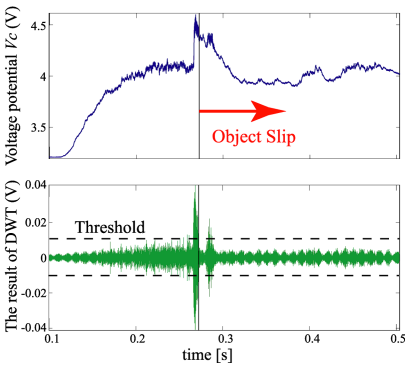

Fig. 9. Analysis results: DWT for object slip. Initial normal force is $2N$

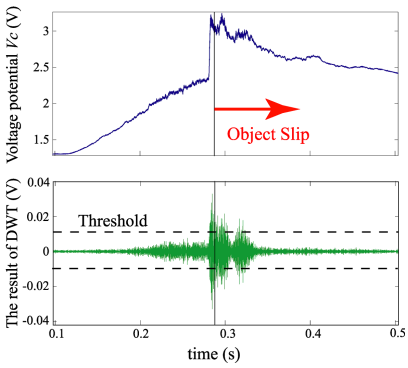

Fig. 10. Analysis results: DWT for object slip. Initial normal force is $3N$

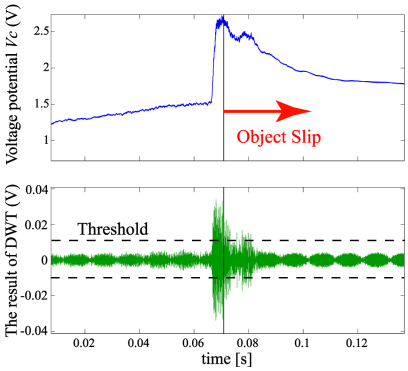

Fig. 11. Analysis results: DWT for the object slip. Initial normal force is $4N$

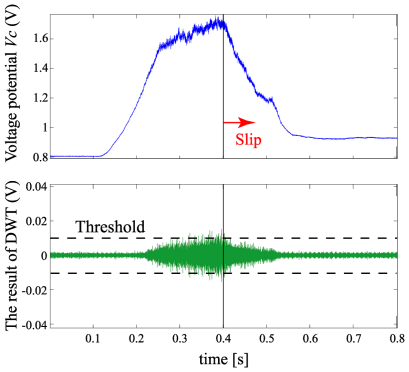

Fig. 12. Analysis results: DWT for object slip. Sliding object is cloth.

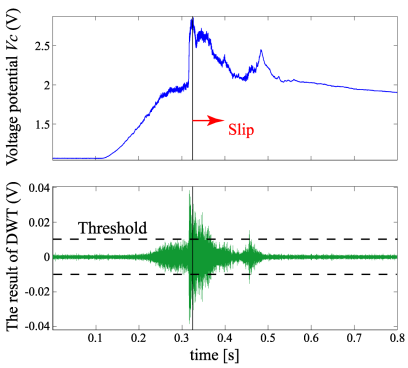

Fig. 13. Analysis results: DWT for object slip. Sliding object is wood.

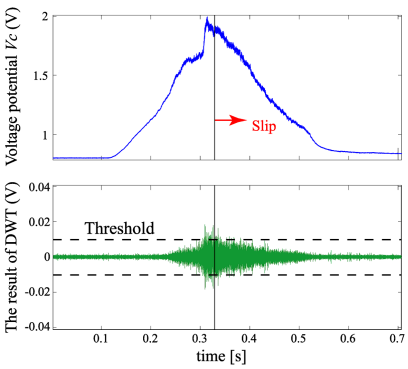

Fig. 14. Analysis results: DWT for object slip. Sliding object is paper.

This parallel hand moved along one axis in the direction of the arrow shown in Fig. 15 and could execute position control. Moreover, the control cycle of this parallel hand was 10 ms. We installed the slip sensors in the right and left parallel fingers. The object was held by these fingers. The slip sensors output was fed back to the parallel hand, and the grip force was adjusted in proportion to the weight of the object. To measure the change in the gripping force used by the parallel hand, a six-axis sensor was installed in the right finger. We adopted the algorithm proposed in the preceding section for initial slip detection.

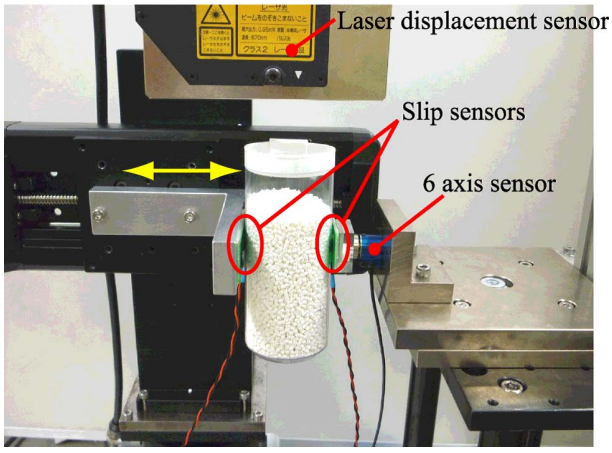

Fig. 15. Parallel hand with installed slip sensors

In this experiment, we performed the following two operations, and confirmed the operation of the sensor.

M1: After an empty glass (made of PET) is gripped with minimal force, minute plastic particles are poured into the glass and the weight is increased. The slip sensor reacts when the object seems to slip, and the grip force is strengthened.

M2: The parallel hand decreases the gripping force, and when the slip sensor detects the initial slip of the glass, the parallel hand strengthens the gripping force slightly. By repeating this operation, the parallel hand can hold the object while applying minimal force.

The control algorithm is simple. The gripping force is strengthened depending on the output from the slip sensor. We use only the output from the slip sensor for the gripping force adjustment algorithm, not output from the six-axis sensor.

The results for motion 1 and motion 2 are shown in Fig. 16 and Fig. 17, respectively. The upper graph shows the gripping force applied by the parallel hand as measured by the six-axis sensor. The middle graph shows the DWT of the voltage signal from the V_c terminal, and the lower graph shows the position of the glass as measured with a laser displacement sensor. As can be seen from the results for motion 1 (Fig. 16), the grip force of the hand was adjusted when the slip sensor detected the initial slip of the object. The output of the

laser displacement sensor hardly changed. Thus, the parallel hand succeeded in gripping an object with varying weight.

Next, as shown from the results for motion 2 (Fig. 17), when the grip force decreased and the object began to slip, the parallel hand reacted based on the output from the sensor: the grip force was slightly increased and the object was prevented from slipping. The displacement of the glass was only 0.5 *mm* as measured with the laser displacement sensor. For several minutes, the parallel hand was able continue holding the object without dropping it.

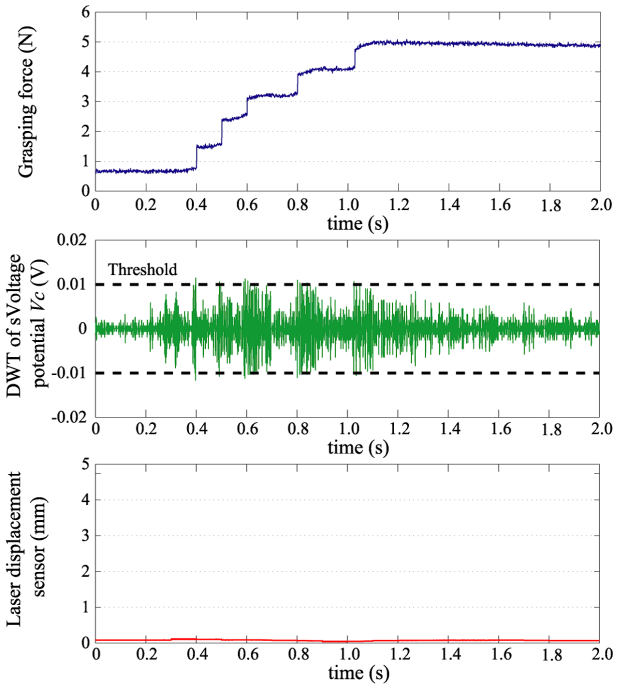

Fig. 16. Motion 1: increasing gripping force while holding an object with increasing weight

VI. CONCLUSIONS AND FUTURE WORK

We have produced a simple slip sensor that exploits the characteristics of pressure conductive rubber. When an object is slid over the sensor, a complex output signal is generated immediately before the object slips. Thus, we performed frequency analysis of this complex output signal by using a CWT. As a result, we found that a frequency component of several kHz was contained in the signal, and that the frequency of this component was about one order of magnitude higher than that for a change in the normal force. Then, we proposed an algorithm for separating information on object slip from the output of the slip sensor, and determined that the change in the normal force could be distinguished by its differing frequency components. We extracted the frequency components for object slip by using DWT as a high-pass filter. As a result, we found that object slip and change in the normal force could be distinguished by setting the threshold to the wavelet coefficient from DWT (level1). Finally, we installed the slip sensor in a parallel hand and performed experiments on the adjustment of gripping force. The parallel hand successfully performed two operations, thus demonstrating the utility of the sensor.

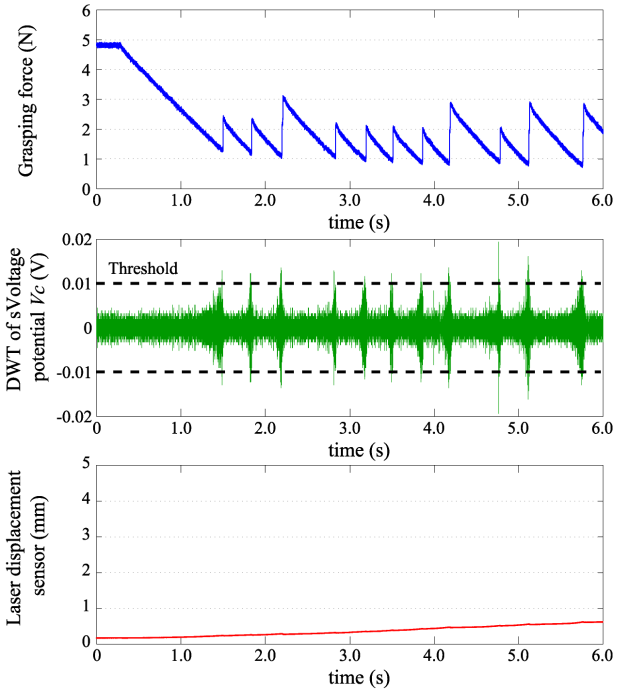

Fig. 17. Motion 2: incrementally decreasing gripping force and then increasing gripping force when the object slip is detected

In the future, we will investigate the most suitable signal processing techniques, and consider the effects of electrode placement, the type of pressure conductive rubber, and the friction coefficient of the object. In addition, we will install this slip sensor in a multi-fingered robot hand.

REFERENCES

[1] R.S. Johanson, G. Westling, *Roles of Glabrous Skin Receptors and Sensorimotor Memory in Automatic Control of Precision Grip when Lifting Rougher or More Slippery Objects*, Exp. Brain Res., Vol. 56, pp. 550-564, 1984

[2] M.R. Trembly, M.R. Cutkosky *Estimating Friction Using Incipient Slip Sensing During a Manipuration Task* , Proc. IEEE Int. Conf. on Robotics and Automation, pp. 429-434, 1993

[3] J.S. Son, E.A. Monteverde and R.D. Howe, *A Tactile Sensor for Localizing Transient Events in Manipulation*, Proc. IEEE Int. Conf. on Robotics and Automation, pp. 471-476, 1994

[4] T. Maeno, K. Kobayashi, N. Yamazaki*Relationship between Structure of Finger Tissue and Location of Tactile Receptors*, JSME Trans., Series C, Vol. 63, No. 607, pp. 881-888, 1997 (in Japanese)

[5] Y. Koda, T. Maeno, *Grasping Force Control in Master-Slave System with Partial Slip Sensor*, Proc. IEEE/RSJ Int. Conf. on Intelligent Robots and Systems, pp. 4641-4646, 2004

[6] H. Shinoda, S. Sasaki, K. Nakamura, *Instantaneous Evaluation of Friction Based on ARTC Tactile Sensor*, Proc. IEEE Int. Conf. on Robotics and Automation, Vol. 3, pp. 2173-2178, 2000

[7] K. Noda, I. Shimoyama, *A Shear Stress Sensing for Robot Hands -Orthogonal Arrayed Piezoresistive Cantilevers Standing in Elastic Material-*, pp. 63-66, HAPTICS' 06

[8] S. Teshigawara, M. Ishikawa, M. Shimojo, *Development of High Speed and High Sensitivity Slip Sensor*, Proc. IEEE Int. Conf. on Intelligent Robots and Systems, pp. 47-52, 2008

[9] S. Teshigawara, K. Tadakuma, M. Aiguo, M. Ishikawa, M. Shimojo, *Development of High-Sensitivity Slip Sensor Using Special Characteristics of Pressure Conductive Rubber*, Proc. IEEE Int. Conf. on Robotics and Automation, pp. 3289-3294, 2009

[10] J.J. Benedetto and M.W. Frazier, *WAVELETS: Mathematics and Applications*, CRC-Press 1993

[11] M. Vetterli and J. Kovacevic, *Wavelets and Subband Coding*, Prentice Hall PTR, 1995